A Study of a Novel Pressure Relief Valve for High-energy Internal Arcing Faults Protection on Ultra-high Voltage Power Transformers

Luo Liang[1], Wang Ke[2,*], Li Jiaxi[2], Zhang Shuqi[2], Zhao Yikun[2]

[1]School of Mechanical Engineering, Hefei University of Technology, Hefei 230000, China
[2]China Electric Power Research Institute, Beijing 100192, China

Abstract: An internal arcing fault in an ultra-high voltage power transformer can release several tens of megajoules of energy within tens of milliseconds, generating severe pressure shocks that pose a significant threat to transformer safety. Effective and efficient pressure relief is essential to enhance the transformer's arc containment capability. However, conventional pressure relief valves available on the market often fall short of protection requirements due to limitations in venting capacity and structural strength. To address this issue, this study proposes a novel pressure relief valve design featuring a significantly larger venting area and an innovative valve disk opening mechanism. First, the working principle and key characteristics of the new valve are described in detail. Subsequently, both structural and fluid dynamics analyses are performed to validate the design. A prototype valve is manufactured and evaluated through equivalent arcing tests and simulations using a small-scale transformer tank. The rolling opening mechanism improves opening efficiency and reduces the weight of individual disks. Moreover, the new valve exhibits a fourfold increase in oil flow rate compared to a valve with 172 mm flange diameter. During arcing tests, the valve operates effectively and reseals successfully, allowing for potential reuse. The tank's maximum and total deformation confirm that a single developed valve provides superior venting performance compared to two smaller valves under identical arcing conditions. This study offers a valuable protective solution for high-energy internal arcing faults in power transformers.

Keywords: UHV Transformer; Pressure Relief Valve; Disk Opening Mode; Internal Arcing Fault; Arcing Experiment

DOI: 10.57237/j.mse.2025.02.001

1 Introduction

Power transformers serve as core components of electrical grids, facilitating the generation, transmission, and end-use of electric power. Ultra-high voltage (UHV) transformers are particularly critical due to their role in efficient long-distance electricity transmission and power regulation [1, 2]. Hundreds of such transformers are already in operation in China's power grid, with many more expected to enter service in the near future.

Internal arcing faults represent one of the most severe and destructive failure modes in power transformers, having been reported worldwide across various voltage levels [3, 4]. During an internal arcing fault, substantial energy is deposited into the insulation oil, causing rapid physical and chemical decomposition of the surrounding insulating oil into gases [5]. The abrupt gas expansion and significant density difference between the generated gases and the oil

Funding: SGCC (Grant No. 5500-202356358A-2-1-ZX).

*Corresponding author: Wang Ke, wangke1@epri.sgcc.com.cn

Received: 7 December 2025; Accepted: 24 December 2025; Published Online: 30 December 2025 http://www.mechscieng.com

create intense pressure shocks [6]. Conventional transformer tanks are generally unable to withstand such overpressure conditions [7]. Moreover, higher voltage levels typically lead to greater energy deposition and more violent pressure shocks, significantly increasing the risk of structural failure in UHV transformers [8].

While internal arcing faults are directly caused by degraded insulation performance of the oil, which can result from multiple factors, and such faults are largely unpredictable and unavoidable [9]. As a result, various protection technologies have been developed [10]. Electrical protection schemes, for instance, monitoring electrical parameters and interrupting the current as quickly as possible, have been developed and applied [11, 12]. However, even modern interrupting devices require several tens of milliseconds to operate, during which time tens of megajoules of energy may be injected into the oil.

Designing transformer tanks as pressure vessels capable of withstanding arcing-induced peak pressure shocks is impractical [13]. This would require wall thickness to increase by an order of magnitude, leading to tank volumes and weights that exceed transportation limits and prove economically unfeasible. Therefore, effective pressure relief is essential for arcing fault protection [14].

Venting area is a key factor influencing pressure relief efficiency [15, 16]. Conventional pressure relief valves (PRVs) used on UHV transformers typically have flange port diameters of 133 mm and 172 mm [17, 18]. Compared to the dimensions of a UHV transformer tank which is roughly 10 meters in length and 4 meters in width, such venting areas are too small to provide adequate protection against high-energy arcing faults. Additionally, the common practice of mounting PRVs diagonally on the transformer cover reduces their effectiveness due to the increased distance from the arc location.

Response speed is another critical parameter for effective pressure relief [19]. However, the inertia of a valve disk can delay the opening action. While enlarging the disk diameter increases venting area, it also increases disk weight, which in turn can reduce opening efficiency [20, 21]. These limitations highlight the need for new PRV designs.

A combined valve–membrane relief device has been developed to leverage the advantages of both PRVs and rupture membranes [22]. Under moderate overpressure, it functions as a conventional PRV, while under extreme pressure, the disk ruptures and acts as a burst membrane to accelerate pressure release. However, this approach results in a permanently open vent and introduces a subsequent fire hazard. Alternatively, simply grouping several small conventional PRVs can increase the total venting area. Yet, this approach often leads to unstable and non-synchronized disk opening, where interactions between adjacent disks can cause mutual interference, compromising both reliable opening and proper resealing.

To address these challenges, this study presents a novel PRV design with an enlarged flange area and a rolling opening mechanism. The working principle and detailed design of the valve are first introduced. Computational fluid dynamics (CFD) and finite element method (FEM) analyses are then employed to investigate and optimize the fluid and structural behavior of the valve. Finally, equivalent arcing tests and simulations are carried out using a prototype valve for validation. This study provides a practical solution to high-energy arcing fault protection.

2 Principle and Design

In conventional direct spring-loaded disc pressure relief valves, the pressure shock must drive the entire disc to open. A major limitation of larger valves is their slower response, which results from the increased mass of the disc. Moreover, complete separation of the disc from the flange compromises movement stability and jeopardizes resealing reliability.

In contrast, the proposed design employs a rolling-opening mechanism, where each disc is hinged along one edge to the flange. Furthermore, multiple discs are arranged symmetrically in an array, which not only reduces the individual mass of each disc but also allows the total venting area to equal the combined area of all discs.

As illustrated in Figure 1, the novel valve consists of four discs arranged in a circular configuration. Each disc is hinged to the valve housing and held in place by springs. When a pressure shock acts on the discs, they pivot around the hinge in a rolling motion. This rolling mechanism, combined with a larger valve body, requires only a small portion of the disc area to be connected to the springs. As a result, the remaining area can be structurally reinforced with ribs, leading to an overall reduction in disc weight compared to conventional pressure relief valves where major disc contacts with springs. This reinforcement enables the use of aluminum instead of steel for the discs, further decreasing disk weight.

Figure 2 displays the detailed design of the new valve and reinforced disk. Additionally, a plastic buffer is installed at the top of each disc to prevent over-rotation and absorb rigid impact. The discs can achieve a maximum rolling angle of up to 75°, significantly increasing the effective venting area. A micro-switch is incorporated to generate a trigger signal, and the valve outlets, located on the top, are equipped with two symmetrically arranged self-operating gates that protect the internal components from environmental contaminants at normal condition.

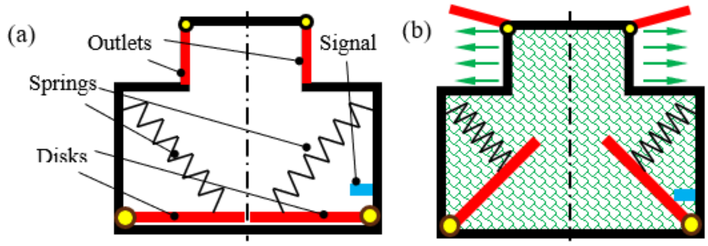

Figure 1 Principle of the new valve (a) closed state and (b) opened state

Each disk is in a shape of a quarter of a circle, and thus its dynamic response is expressed in Eq. (1).

$$\dot{\omega} = \begin{cases} 0 & M_p - M_s \le 0 \\ \frac{M_p - M_s}{I} = \frac{pR^3}{6\sqrt{2}I} - \frac{k\left(d_0 + \frac{R}{2}\sin\theta\right)\frac{R}{2}}{I} = \frac{\sqrt{2}pR}{m} - \left(\frac{6kd_0}{mR} + \frac{3k\sin\theta}{m}\right) & M_p - M_s > 0 \end{cases} \quad (1)$$

where $\dot{\omega}$ and θ are disk rotation acceleration and angle respectively, M_p and M_s are moment of pressure shock and spring force respectively, p is pressure, R is disk radius, m is disk mass, I is disk rotational inertia, k is spring stiffness, and d_0 is spring precompression distance.

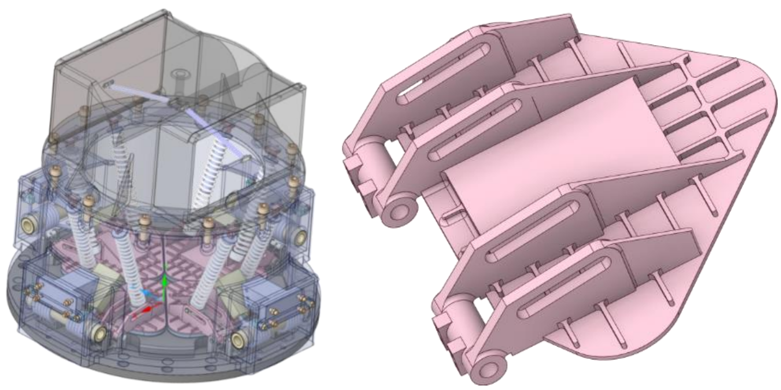

(a) (b)

Figure 2 Design of the new valve (a) total view and (b) reinforced disk

3 Structure Analysis

Withstanding pressure shocks and maintaining structural integrity are fundamental requirements for the valve. In this study, the valve design was validated through static finite element analysis (FEA) under an equivalent constant pressure. During an arcing event, peak pressure can be as high as several tens of mega pascals, however, the peak shock only lasts a few milliseconds and won't damage the structure. Additionally, due to pressure relief, pressure on the valve body is smaller than that on other part of the tank. Thus, a uniform static pressure of 4 MPa was applied to the valve, and the deformation and stress distribution of its key components were evaluated. Beyond ensuring structural integrity, the total deformation of the valve must remain below a critical threshold to guarantee reliable resealing after an internal arcing fault.

The valve assembly was appropriately simplified for simulation, while retaining all major structural components—including the flange, valve disks, and valve cover. In accordance with the actual installation conditions, the bottom surface of the flange, which interfaces with the transformer tank cover, was defined as a fixed support. The static pressure load was applied uniformly to both the flange and the valve disks. Figure 3 illustrates the FEA model of the valve and the corresponding boundary conditions. The entire assembly was discretized using high-quality solid elements to ensure computational accuracy.

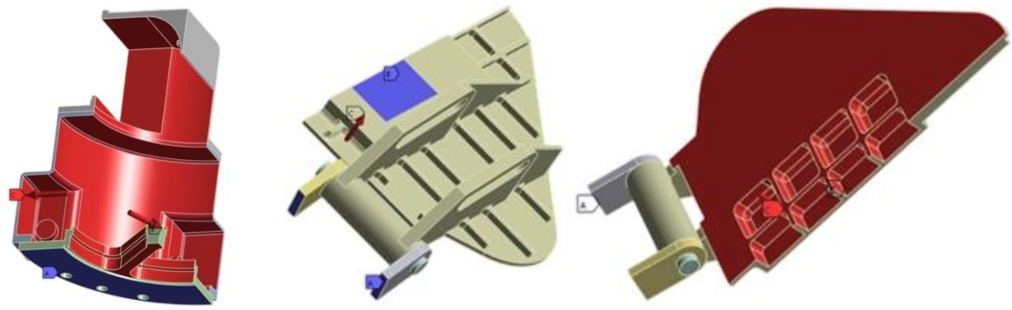

(a) (b)

Figure 3 FEM model and boundary conditions

Figure 4 displays the overall deformation results of the valve. With structural reinforcement applied to the valve disks, the maximum deformation observed on the aluminum disk remains below 8.2 mm. Since the maximum stress in the disk does not exceed its yield strength, the deformation is entirely elastic and will recover fully upon pressure release. This ensures that the valve can achieve effective resealing after operation.

The housing, meanwhile, exhibits a maximum deformation of approximately 14.5 mm, located at the outlet region. This deformation remains within the acceptable structural limits, confirming that the main valve body can withstand the pressure shock without failure.

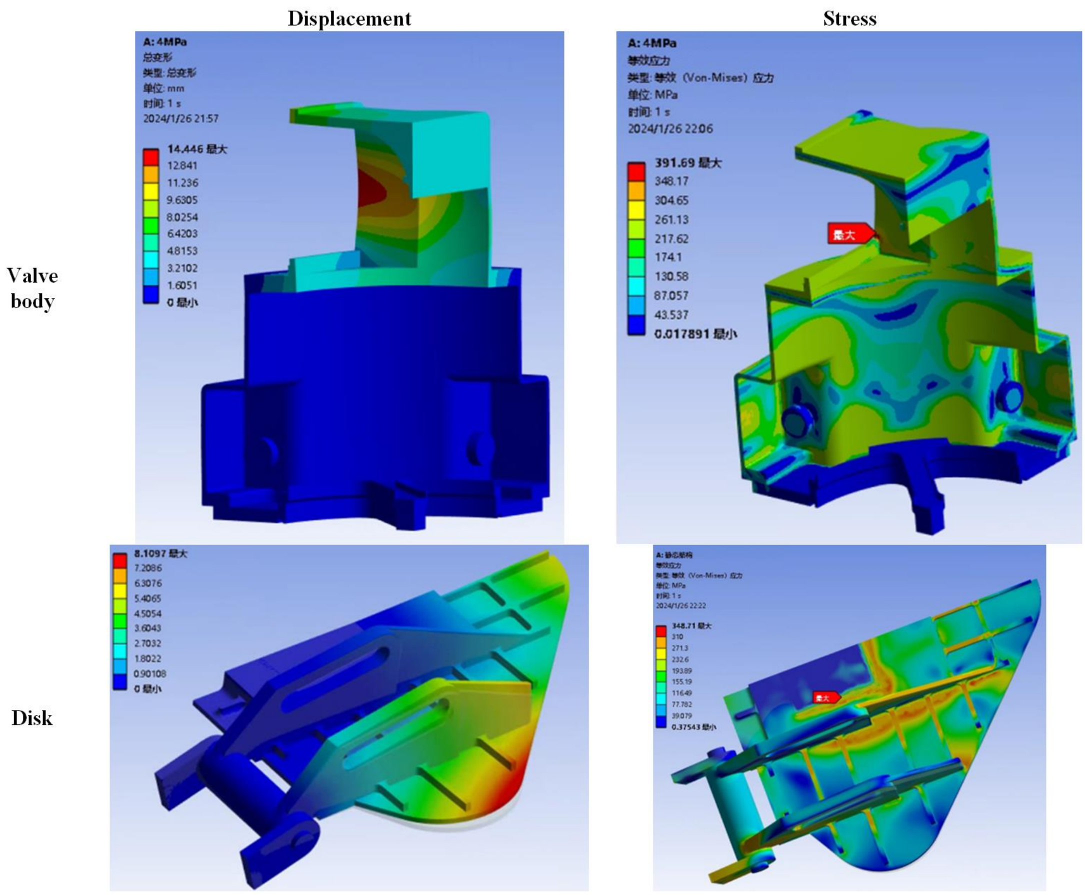

Figure 4 Stress and displacement of the valve body and disk

4 CFD Analysis

The pressure relief capacity of the valve was investigated and compared using computational fluid dynamics (CFD). A quarter-section of the valve model was simulated with symmetric boundary conditions to reduce computational cost. A transient analysis was performed with the disks in the fully open position, using an inlet pressure profile derived from experimental data.

The fluid domain was discretized with polyhedral elements, while layered mesh refinement was applied to the disks and side walls of the valve to enhance resolution and improve calculation accuracy. Figure 5 illustrates the resulting mesh model used for the simulation.

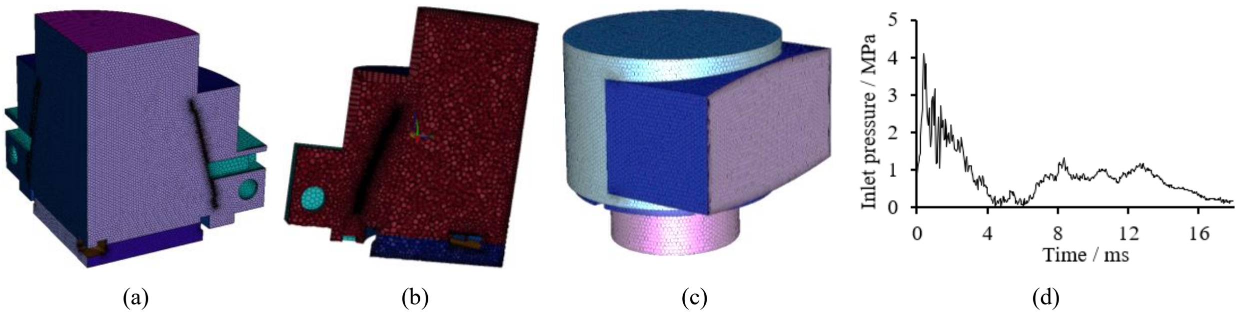

Figure 5 CFD model of (a) developed valve, (b) cross-section view, (c) commercial valve, and (d) inlet pressure curve

The maximum pressure in the developed valve is 1 MPa compared to 2.1 MPa in a commercial valve with a diameter of 172 mm. This also validates that static pressure assumption in the structural analysis is reasonable. The oil flow velocity is much slower than the commercial valve. Moreover, there is not vortex flow in the new valve indicating a smooth flow in the new valve.

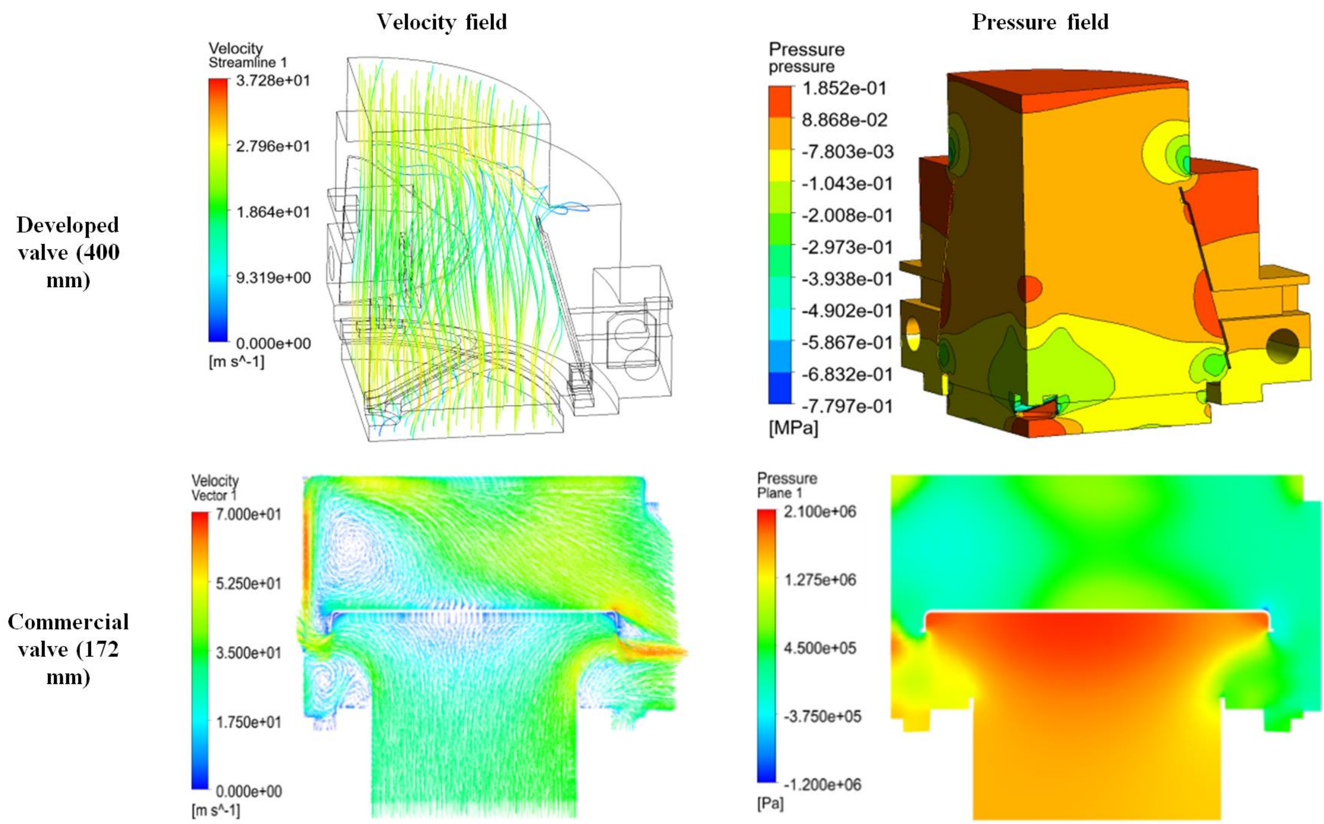

Figure 6 Flow field and pressure field of the valve

For comparison, a commercial pressure relief valve and a rupture disk, both with a flange diameter of 172 mm, were also modeled under the same inlet pressure condition. Figure 7 illustrates the comparative flow rates of the proposed valve, the commercial valve, and the rupture disk. As expected, the rupture disk exhibits superior pressure relief performance compared to a conventional PRV of the same flange diameter, due to the absence of an obstructive disk structure. Furthermore, the results confirm that increasing the flange area significantly enhances venting capacity by fourfold.

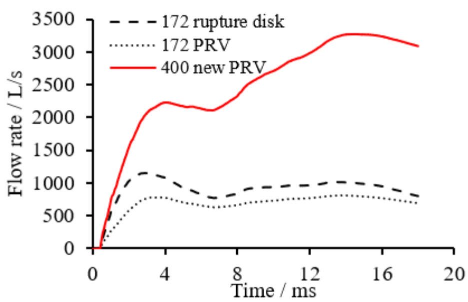

Figure 7 Flow rate of the valves and rupture disk

5 Prototyping

Both the structural and CFD analyses confirm that the developed valve exhibits satisfactory performance, leading to the fabrication of a prototype for experimental validation under arcing conditions. Figure 8 presents the key components and the fully assembled view of the proposed valve. The main structural parts are constructed from Q235 steel, while the reinforced disks are manufactured from 6061 aluminum alloy. Rubber seals are installed between the flange and disks to ensure effective sealing.

To maintain balanced movement during operation, dual springs are arranged in parallel for each disk. These springs compress and pivot synchronously as the disks roll open. Additionally, rollers are incorporated at the spring connections to facilitate smooth rotation and compression throughout the opening and closing cycles.

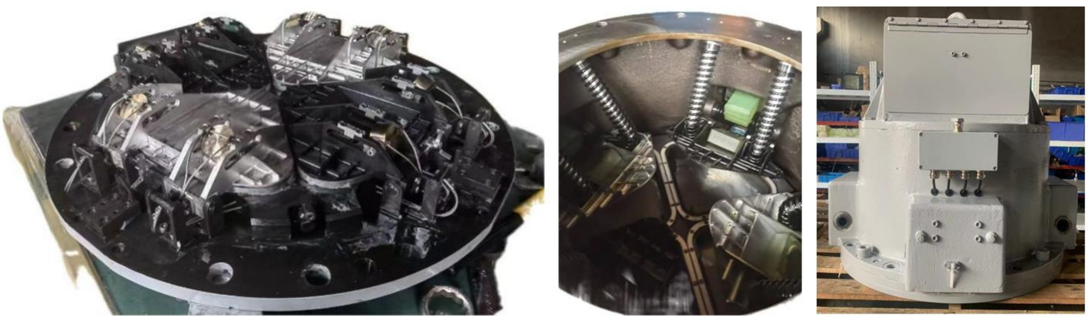

(a) (b) (c)

Figure 8 Prototype of the new valve with its key components (a) flange and closed disks, (b) opened disks and (c) valve assembly

6 Equivalent Arcing Experiments

A small-scale experimental transformer tank with a length of 3.5 m and a width of 1.5 m was designed and fabricated to conduct equivalent arcing tests under controlled conditions, as shown in Figure 9 and Figure 10. The developed valve and two traditional small PRV with a 172 mm flange diameter were installed separately on the test tank and subjected to identical arcing fault scenarios. An arcing energy of 3.7 MJ is deposited in each experiment.

The developed valve demonstrated excellent performance during the arcing experiment. Throughout the pressure relief process, no ignition or fire was observed. After the arcing, the valve successfully resealed itself, preventing any further leakage of insulating oil and thereby eliminating the risk of subsequent fire and explosion. As shown in Figure 11(b), post-experiment inspection confirmed that the valve remained structurally intact, allowing for potential reuse in future applications.

As shown in Figure 11, tank strain measurements indicate that the developed valve significantly reduces tank deformation, as reflected by the measured strain values, compared to the smaller valve. Lower strain levels in the tank suggest improved pressure relief capacity of the valve and a reduced risk of tank fracture.

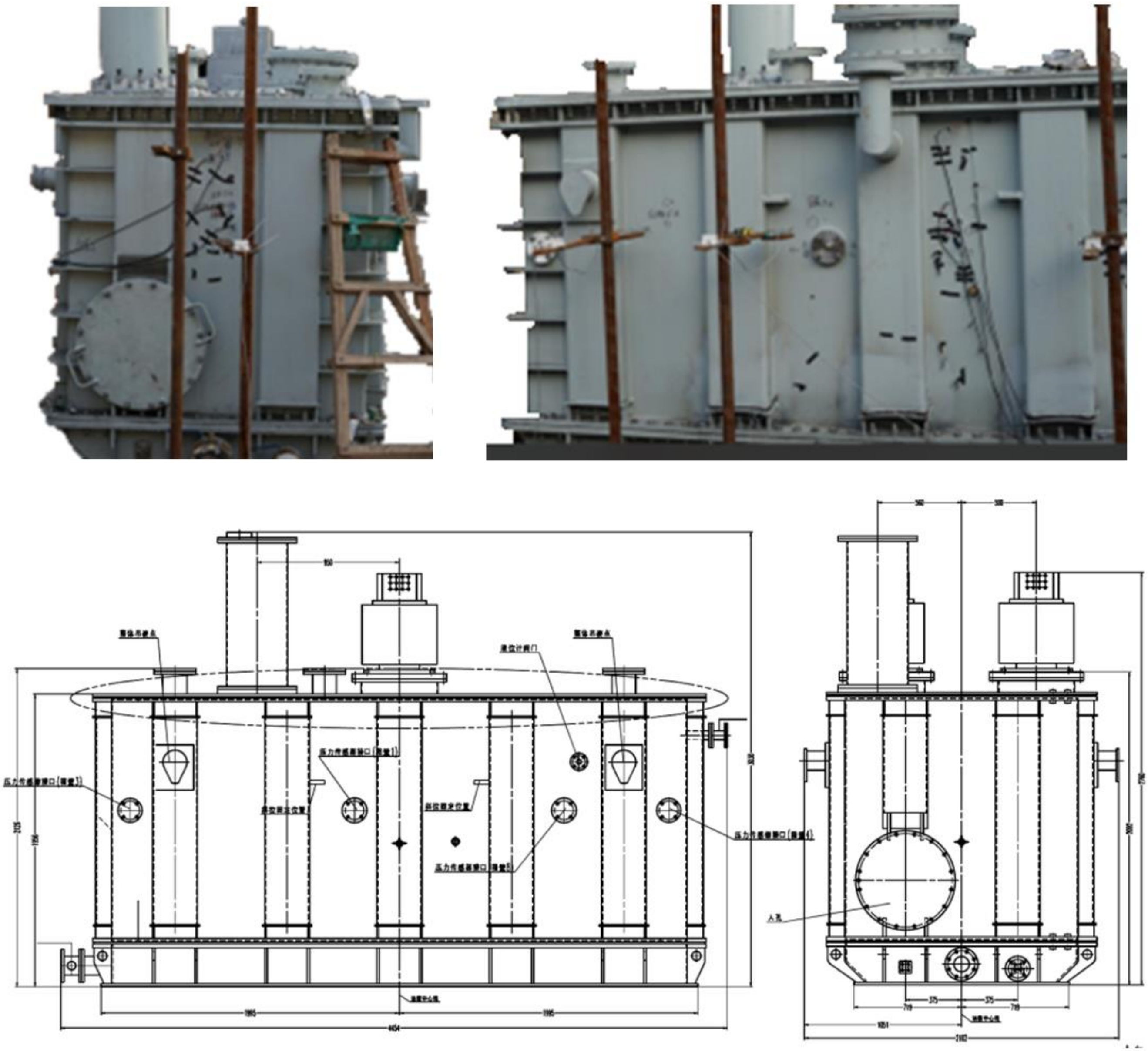

Figure 9 Small-scale experimental tank

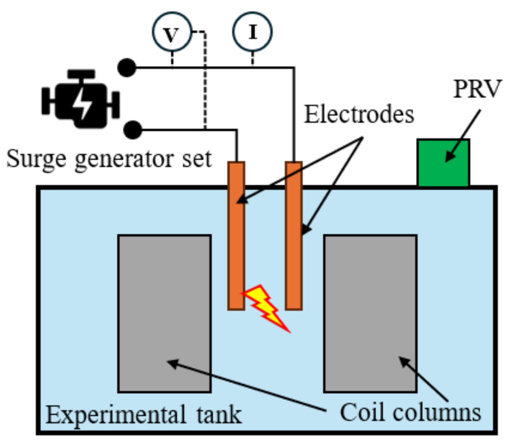

Figure 10 Principle of equivalent arcing experiments

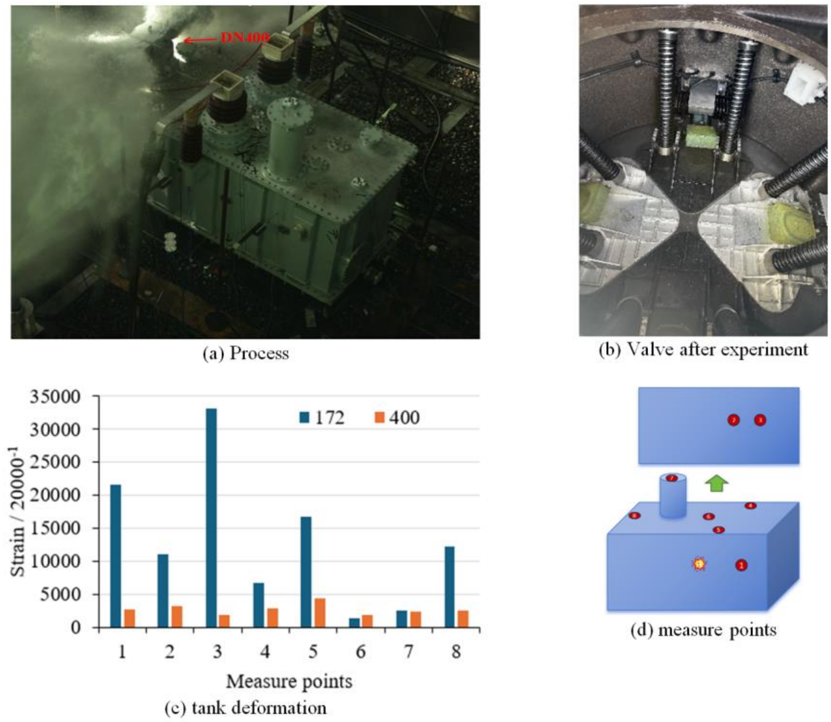

Figure 11 Arcing experimental results

7 Arcing Simulation

A further validation of the developed valve and its pressure relief performance is conducted numerically based on an experimental transformer tank. Figure 12 shows the tank and its FE model. The tank body is modeled with shell elements following Johnson-cook material constitutive model. The copper coils and iron cores are all considered via solid elements with an elastic material model. Initially, the tank is filled with insulation oil governed by Gruneisen equation of state (Eq. (2)). The arcing source is simplified as a TNT explosive and ignited at the start of simulation. The TNT provides a pressure shock which can also presents propagation in insulation oil as arcing pressure shock. The entire simulation accounts 60 ms after ignition of the TNT, when the tank structure plastic deformation is completed. To compared the effects of the developed valve, a small valve with a flange diameter of 172 mm is utilized on the same experimental tank in the arcing experiment with the same arcing energy.

$$p = \frac{\rho_0 C^2 \mu\left[1+\left(1-\frac{\gamma_0}{2}\right)\mu-\frac{a}{2}\mu^2\right]}{\left[1-(S_1-1)\mu-S_2\frac{\mu^2}{\mu+1}-S_3\frac{\mu^3}{(\mu+1)^2}\right]^2}+(\gamma_0+a\mu)E \quad (2)$$

where P is oil pressure, C is the intercept of the curve (in velocity units), S_1, S_2 and S_3 are the unitless coefficients of the slope of the curve, γ_0 is the unitless Gruneisen gamma, a is the unitless, first order volume correction to γ_0, E denotes the internal energy, and

$$\mu = \frac{\rho}{\rho_0} - 1 \quad (3)$$

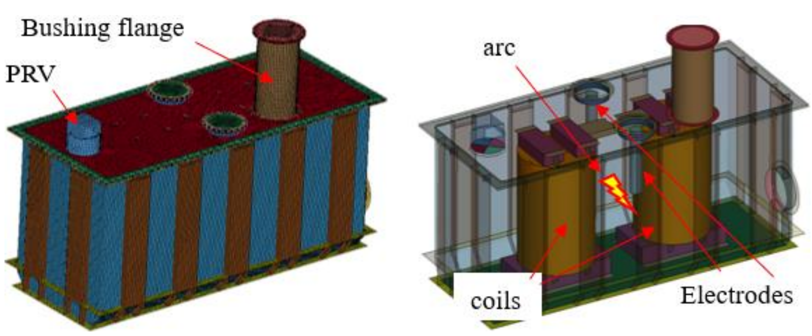

Figure 12 Experimental tank simulation model

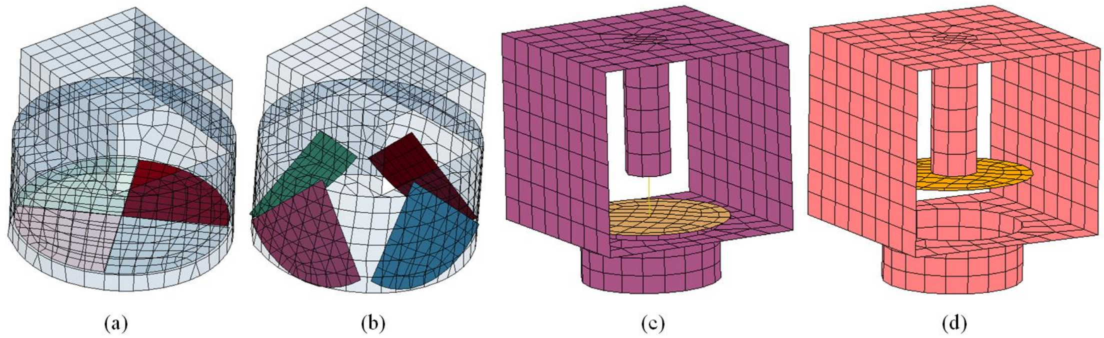

Figure 13 FE model of the developed pressure relief valve (a) closed state and (b) fully opened state, and a traditionally small valve (c) closed state and (d) fully opened state

Figure 14 compares the valve disk movement of the valves. With the developed valve, the tank deformation peaks at the top cover of 24.5 mm being smaller than that of the tank with two small PRVs of 29.5 mm. Total tank plastic deformation energy, shown in Figure 15, also proves that the developed valve shows better relief effect and results in less damage to the tank.

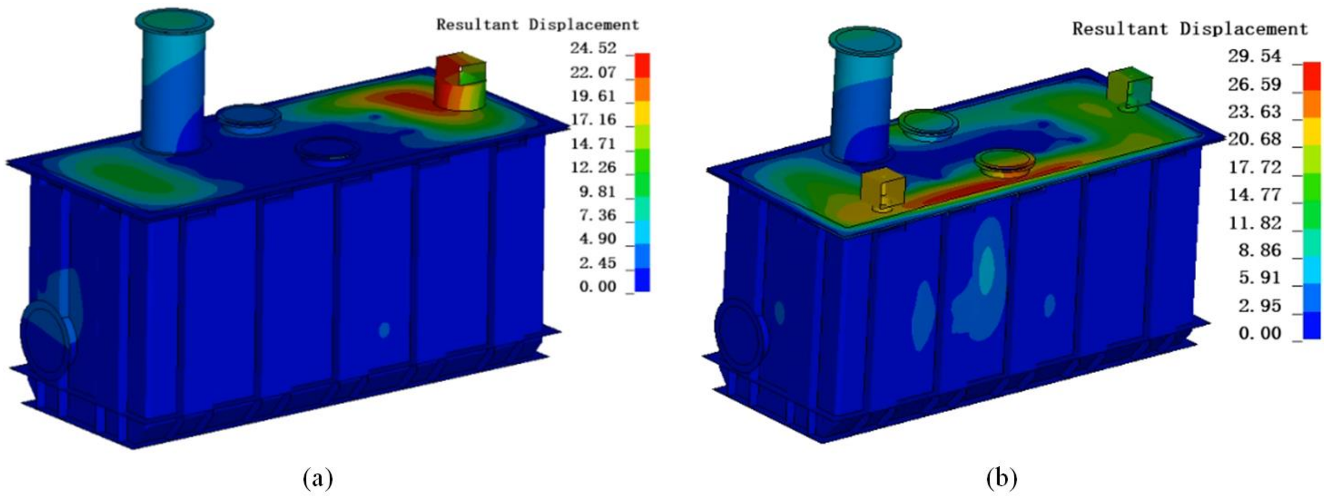

Figure 14 Tank final deformation (a) with the developed valve and (b) with two small traditional PRVs

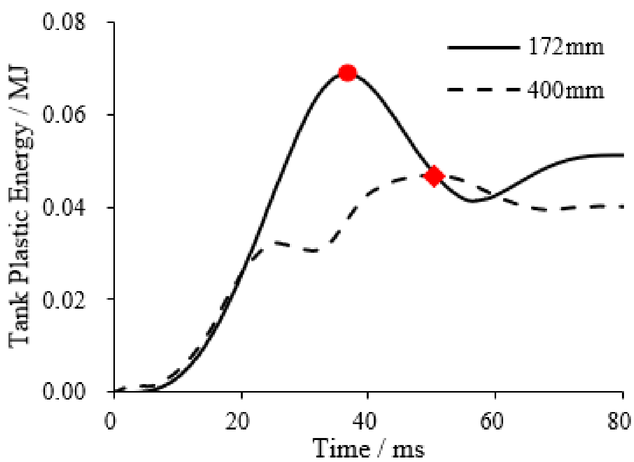

Figure 15 Tank plastic deformation energy

8 Conclusion

A novel PRV featuring a 400 mm flange diameter and a rolling-opening mechanism has been successfully designed and developed. Compared to conventional pressure relief valves, the rolling-opening mode enhances dynamic response and significantly increases the effective venting area.

Structural analysis confirms that the valve withstands static pressures up to 4 MPa without experiencing deformations that would compromise its resealing capability. CFD simulations demonstrate a fourfold improvement in venting efficiency relative to a conventional valve with a 172 mm flange diameter.

Arcing tests were conducted on a small-scale transformer tank equipped with different valve configurations. The developed valve performed reliably throughout the arcing event, successfully resealing the tank. Structural inspection confirmed its integrity, indicating potential for reuse. Under identical arcing conditions, the use of two conventional 172 mm PRVs resulted in higher tank deformation, further validating the superior relief performance of the proposed design.

A strong fluid-structure interaction simulation of the equivalent arcing experimental conditions was employed to evaluate venting effectiveness. The final deformation of the test tank fitted with the developed valve was notably smaller than that observed with two smaller valves, demonstrating its enhanced protection capacity.

This study provides a practical and effective solution for mitigating high-energy internal arcing faults in power transformers.

Acknowledgments

This work is financially supported by SGCC (Grant No. 5500-202356358A-2-1-ZX). The authors are grateful to Mr. Shaojie Wang for his assistance with the design and engineering drawings.

References

[1] Jia, Y., Luo, X., Ji, S., Zhao, D., Qiu, Z., and Li, S., 2025, “Pressure and Stress Characteristics of Transformer Tank with Power-Frequency Arc Fault in Oil,” Thin-Walled Structures, 210, p. 112986. https://doi.org/10.1016/j.tws.2025.112986

[2] Brodeur, S., Lê, V. N., and Champliaud, H., 2021, “A Nonlinear Finite-Element Analysis Tool to Prevent Rupture of Power Transformer Tank,” Sustainability, 13(3), p. 1048. https://doi.org/10.3390/su13031048

[3] 2016, “IEEE Guide for Tank Rupture Mitigation of Liquid-Immersed Power Transformers and Reactors,” (C57.156TM-2016). https://doi.org/10.1109/IEEESTD.2016.7792305

[4] 2013, *Guide for Transformer Fire Safety Practices*, CIGRE.

[5] Mu, Z., Wang, C., Meng, Y., and Ding, W., 2025, “Gas Generation and Pressure Characteristics of Arcing Faults in Transformer Oil,” IEEE Transactions on Power Delivery, 40(4), pp. 2048–2058. https://doi.org/10.1109/TPWRD.2025.3567738

[6] Yao, H., Lv, K., Lou, Z., Xing, M., Qin, H., Song, H., Lv, Z., Wang, D., Wang, Z., and Ren, W., 2023, “Simulation Study on Oil Pressure Problems Caused by Internal Faults in Oil-Immersed Transformers,” Process Safety and Environmental Protection, 175, pp. 190–198. https://doi.org/10.1016/j.psep.2023.05.053

[7] Brodeur, S., and Dastous, J.-B., 2020, “Design and Testing of an Arc Resistant Power Transformer Tank,” IEEE Transactions on Power Delivery, 35(2), pp. 699–706. https://doi.org/10.1109/TPWRD.2019.2922505

[8] 2018, “IEEE Standard for Requirements for Distribution Transformer Tank Pressure Coordination.”. in IEEE Std C57.12.39-2017, pp.1-23, https://doi.org/10.1109/IEEESTD.2018.8353821

[9] Ham, J. K., Lee, J. Y., Yang, J. C., and Lee, J. K., 2010, “Tank Rupture Prevention Technology for a Large Power Transformer,” *CIGRE Session*. Available: https://www.zhangqiaokeyan.com/academic-conference-foreign_meeting-268594_thesis/0705015223370.html

[10] Chothani, N., Raichura, M., and Patel, D., 2023, “An Overview of the Protection of Power Transformers,” *Advancement in Power Transformer Infrastructure and Digital Protection*, N. Chothani, M. Raichura, and D. Patel, eds., Springer Nature, Singapore, pp. 27–69. https://doi.org/10.1007/978-981-99-3870-4_2

[11] Roseberg, T., Jankovic, I., and Hedding, R., 2017, “Transformer Tank Rupture - A Protection Engineer’s Challenge,” *2017 70th Annual Conference for Protective Relay Engineers (CPRE)*, College Station, TX, USA, pp. 1–29. https://doi.org/10.1109/CPRE.2017.8090054

[12] Khan, M. R., 2018, “A Literature Review: Traditional and Advanced Protection Schemes of Power Transformer,” *JETIR*. 5(4), p.136-139. Available: https://www.jetir.org/view?paper=JETIREP06034

[13] Brady, R., Muller, S., Petrovan B. M., Perigaud, G., and Landis, B., 2010, “Prevention of Transformer Tank Explosion: Part 3—Design of Efficient Protections Using Numerical Simulations,” American Society of Mechanical Engineers Digital Collection, pp. 667–675. https://doi.org/10.1115/PVP2009-77413

[14] Jia, W., Zhang, J., Zhang, H., Gong, M., Sheng, J., Xing, W., Dong, D., Qu, L., and Song, B., 2022, “Research of Property and Calibrate Method for Pressure Release Device of Power Transformer in the Grid,” J. Phys.: Conf. Ser., 2310(1), p. 012055. https://doi.org/10.1088/1742-6596/2310/1/012055

[15] Iyer, A. P., Goj, A., and Ahmed, O. K., 2018, “Performance of Depressurization Devices to Dynamic Loads Generated by Arcing in Liquid Filled Transformers,” American Society of Mechanical Engineers Digital Collection. https://doi.org/10.1115/PVP2018-84691

[16] Brady, R., Perigaud, G., Muller, S., Petrovan, B. M., and Landis, B., 2009, “Application of a 3D Computer Simulation Tool as a Decision Making Tool for Optimizing Transformer Protection,” *2009 IEEE Power Energy Society General Meeting*, pp. 1–8. https://doi.org/10.1109/PES.2009.5275234

[17] Guo, Z. W., Liu, X. L., Guo, X. J., Liu, C. K., Jing, C., Li, Y., and Tang, M., 2017, “Research on Pressure Relief Technology of Main Transformer in 220KV Indoor Substation,” Applied Mechanics and Materials, 873, pp. 279–284. https://doi.org/10.4028/www.scientific.net/AMM.873.279

[18] Yan, C., Wei, Y., Xu, C., and Zhang, B., 2019, “Experimental Verification and Electromagnetic–Mechanics–Acoustic Field Coupling Analysis of Transformer Pressure Relief Valve Malfunctions Due to External Short-Circuit Faults,” IEEE Transactions on Magnetics, 55(6), pp. 1–4. https://doi.org/10.1109/TMAG.2019.2900660

[19] Xue, Q., Wang, H., Liu, H., Zhang, P., Yang, H., Wang, W., and Yan, C., 2022, “Numerical Investigation of Transformer Pressure Relief Valve Operation Characteristics,” *4th International Conference on Electrical Engineering and Control Technologies, CEECT 2022, December 17, 2022*, Institute of Electrical and Electronics Engineers Inc., Virtual, Online, China, pp. 266–270. https://doi.org/10.1109/CEECT55960.2022.10030724

[20] Luo, L., Li, J., Zhang, N., Wang, K., Zhang, S., and Liang, N., 2022, “Design and Analysis of a New Pressure Relief Valve for Oil-Immersed Electrical Equipment,” Journal of Pressure Vessel Technology, 145(2), p. 021701. https://doi.org/10.1002/prs.12006

[21] Karroud, N. H., Prigent, S., Scheurer, D., Farinati, R., and Magnier, P., 2001, *Pressure Relief Valve Efficiency Calculations by Comparison to the SERGI TRANSFORMER PROTECTOR during Transformer Short-Circuit*, rpisp01a, SEGRI. Available: http://doc.paperpass.com/foreign/rgTech2001185109940.html (Accessed: 22-Apr-2024).

[22] Valenta, L., Černý, I., and Maternik, D. A., 2016, “Power Transformers and Environmental Protection,” IFAC-Papers OnLine, 49(27), pp. 18–22. https://doi.org/10.1016/j.ifacol.2016.10.693